

# Hydrothermal synthesis, structural, Raman, and luminescence studies of $\text{Am}[M(\text{CN})_2]_3 \cdot 3\text{H}_2\text{O}$ and $\text{Nd}[M(\text{CN})_2]_3 \cdot 3\text{H}_2\text{O}$ ( $M = \text{Ag}, \text{Au}$ ): Bimetallic coordination polymers containing both trans-plutonium and transition metal elements

Zerihun Assefa<sup>a,\*</sup>, Katrina Kalachnikova<sup>b</sup>, Richard G. Haire<sup>c</sup>, Richard E. Sykora<sup>b</sup>

<sup>a</sup>Department of Chemistry, North Carolina A&T State University, Greensboro, NC 27411, USA

<sup>b</sup>Department of Chemistry, University of South Alabama, Mobile, AL 36688, USA

<sup>c</sup>Chemical Sciences Division, Oak Ridge National Laboratory, Oak Ridge, TN 37831, USA

Received 21 May 2007; received in revised form 16 August 2007; accepted 31 August 2007

Available online 14 September 2007

## Abstract

The polymeric compounds consisting of the man-made element, americium, and gold and silver dicyanides were prepared under mild hydrothermal conditions at 120 °C. It was found that the americium ion and the transition metal ions are interconnected through cyanide bridging in the compounds. Given the similarities in the radii of americium and neodymium, crystals of the latter were also characterized for comparison purposes. The four compounds are isostructural and crystallize in the hexagonal space group,  $P6_3/mcm$ , with only slight differences in their unit cell parameters. Crystallographic data (MoK $\alpha$ ,  $\lambda = 0.71073 \text{ \AA}$ ):  $\text{Am}[\text{Ag}(\text{CN})_2]_3 \cdot 3\text{H}_2\text{O}$  (**1**),  $a = 6.7205(10) \text{ \AA}$ ,  $c = 18.577(3) \text{ \AA}$ ,  $V = 726.64(19)$ ,  $Z = 2$ ;  $\text{Am}[\text{Au}(\text{CN})_2]_3 \cdot 3\text{H}_2\text{O}$  (**2**),  $a = 6.666(2) \text{ \AA}$ ,  $c = 18.342(3) \text{ \AA}$ ,  $V = 705.9(4)$ ,  $Z = 2$ ;  $\text{Nd}[\text{Ag}(\text{CN})_2]_3 \cdot 3\text{H}_2\text{O}$  (**3**),  $a = 6.7042(4) \text{ \AA}$ ,  $c = 18.6199(14) \text{ \AA}$ ,  $V = 724.77(8)$ ,  $Z = 2$ ; and  $\text{Nd}[\text{Au}(\text{CN})_2]_3 \cdot 3\text{H}_2\text{O}$  (**4**),  $a = 6.6573(13) \text{ \AA}$ ,  $c = 18.431(4) \text{ \AA}$ ,  $V = 707.2(2)$ ,  $Z = 2$ . The coordination around the Am and/or Nd consists of six N-bound  $\text{CN}^-$  groups resulting in a trigonal prismatic arrangement. Three capping oxygen atoms of coordinated water molecules complete the tricapped trigonal prismatic coordination environment, providing a total coordination number of nine for the  $f$ -elements. Raman spectroscopy, which compliments the structural analyses, reveals that the four compounds display strong signals in the  $\nu_{\text{CN}}$  stretching region. When compared with  $\text{KAg}(\text{CN})_2$  or  $\text{KAu}(\text{CN})_2$ , the  $\nu_{\text{CN}}$  stretching frequencies for these compounds blue-shift due to bridging of the dicyanometallate ions with the  $f$ -element ions. There is subsequent reduction in electron density at the cyanide center. Compared with the silver systems, the  $\nu_{\text{CN}}$  frequency appears at higher energy in the gold dicyanide complexes. This shift is consistent with the structural data where the carbon–nitrogen bond distance is found to be shorter in the gold dicyanides.

© 2007 Elsevier Inc. All rights reserved.

**Keyword:** Trans-plutonium complexes; Coordination polymer; Emission; Hydrothermal syntheses

## 1. Introduction

The design and synthesis of self-assembling supramolecular systems is of intense interest as a rational route for generating important functional materials. One facet in this crystal engineering approach is the use of relatively weak-bonding interactions, such as hydrogen bonding [1–5].

cyanide-bridged, bimetallic systems prepared by assembling cyanometallates and transition metal and/or lanthanide building blocks exhibit fascinating structural, magnetic, electrochemical, and magneto-optical properties [6–11]. The importance of metal containing polymers for new materials is quite extensive and Au(I)-, Ag(I)-, and Pt(II)-based polymers are of particular importance because of their unique photophysical properties [12–14].

Gold(I) centers are known to form weakly bonding aurophilic interactions which have strengths that are on the same order-of-magnitude as that for hydrogen bonds [15].

\*Corresponding author. Tel.: +1 336 433 6741; fax: +1 336 334 7124.

E-mail addresses: [zassefa@ncat.edu](mailto:zassefa@ncat.edu) (Z. Assefa), [rsykora@jaguar1.usouthal.edu](mailto:rsykora@jaguar1.usouthal.edu) (R.E. Sykora).

The association usually extends to yield larger oligomers and one- or two-dimensional polymers. In general terms, “aurophilic” bonding of this type is now widely accepted as the most prominent example of a general phenomenon of metallophilicity, and is recognized as a major factor in determining supramolecular structures and properties [16–18]. Hence, the chemistry of Au(I) is satiated with systems that are polymeric by virtue of these Au–Au interactions. In this regard, the linear building block dicyanoaurate,  $[\text{Au}(\text{CN})_2]^-$ , is a convenient unit with which to explore the use of aurophilicity as a supramolecular design element [16–20]. This simple anion has been extensively studied over the years due to its ability to form coordination polymers through cyanide bridging. It can form polymers in a fashion similar to other metal–cyanide anions, where the central Au(I) atom is prone to forming gold–gold bonds both in solution [20–21] and in the solid state [22–26]. Similar structural features are also exhibited in Ag(I) and Pt(II) systems displaying what are known as “argentophilic” and “platinophilic” interactions, respectively.

While a majority of the synthetic procedures of these systems follow conventional solution routes, interest has also been shown in the less-conventional solvothermal techniques. Many homometallic cyanide-bridged copper(I) systems constructed through hydrothermal techniques by using CuCN and aromatic imine ligands as starting materials have been reported recently [27,28]. The first cyanide-bridged bimetallic complex prepared by solvothermal techniques, an Fe(II)–Cu(I) complex, was reported in 2003 by Colacio et al. [29]. Of the vast array of gold complexes reported, an ISI literature search provides  $\text{Pb}[\text{Au}(\text{CN})_2]_2(\text{H}_2\text{O})$  as the only compound synthesized recently using a hydrothermal technique [30].

The synthesis of trans-plutonium compounds, especially as single crystals, is complicated by the limited availability of the materials and restriction on the experimental procedures that can be adapted due to their high radioactivity. Single-crystal X-ray studies in most cases are not possible given the radioactive nature that restricts handling and reduces the stability of the crystals. As a result, most of the potential compounds of these are unexplored due to the special equipment and facilities needed to deal with such materials, as well as crystal deterioration that arises due to self-irradiation.

In this paper, we report an example of a trans-plutonium element linked to a transition metal through cyanide bridging to form a three-dimensional coordination polymeric structure. Only a handful of coordination polymeric compounds have been described involving the transuranium element, neptunium [31,32]. To the best of our knowledge, prior examples of coordination polymers involving the trans-plutonium elements do not exist.

The polymeric compounds between the man-made element, americium, and gold and silver dicyanides were prepared using the less-conventional hydrothermal synthetic procedure. When compared to the more traditional,

slow evaporation technique, the hydrothermal synthetic procedure is especially useful for more-rapid single-crystal growth, which helps counter the internal, radioactive-induced crystal deterioration. The neodymium system is reported for structural comparison, since  $\text{Nd}^{3+}$  has a similar ionic size to that of  $\text{Am}^{3+}$ .

## 2. Experimental Section

### 2.1. Materials and methods

The americium used in these studies was made available through the US Department of Energy.  $\text{Nd}_2\text{O}_3$  (Research Chemicals, 99.9%),  $\text{NdCl}_3$  (Strem Chemicals, 99.9%),  $\text{KAg}(\text{CN})_2$  (Alfa-Aesar, 99.9%), and  $\text{KAu}(\text{CN})_2$  (Alfa-Aesar, 99.99%) were used as received. Triply distilled water was used in all reactions. An aqueous  $\text{AmCl}_3$  solution was prepared by dissolving Am metal in 1 M HCl, evaporating the resulting solution to dryness, and then dissolving the solid product in  $\text{H}_2\text{O}$ . An aqueous solution of  $\text{Nd}(\text{NO}_3)_3$  was prepared by dissolving  $\text{Nd}_2\text{O}_3$  in concentrated  $\text{HNO}_3$ , evaporating the solution to dryness, and then dissolving the resultant solid in  $\text{H}_2\text{O}$ . The isotopic purity of the americium was determined to be  $>99.9\%$   $^{243}\text{Am}$  by mass spectrometric analysis. *It should be noted that special training and experimental facilities are required in order to perform work with highly radioactive transuranium materials, such as americium.* Preparations of the  $\text{Am}[M(\text{CN})_2]_3 \cdot 3\text{H}_2\text{O}$  ( $M = \text{Ag}, \text{Au}$ ) were conducted in glove boxes in accordance with the established policies for handling radioactive materials at the Oak Ridge National Laboratory. To decrease the likelihood of radioactive contamination, the established policies required that americium samples selected for X-ray and spectroscopic analyses be doubly contained.

### 2.2. Syntheses of $\text{Am}[M(\text{CN})_2]_3 \cdot 3\text{H}_2\text{O}$ ( $M = \text{Ag}$ , **1**; $\text{Au}$ , **2**)

The synthesis of  $\text{Am}[\text{Ag}(\text{CN})_2]_3 \cdot 3\text{H}_2\text{O}$ , (**1**), proceeded by adding  $\text{AmCl}_3$  (40  $\mu\text{L}$ , 0.095 M) to a quartz reaction vessel that had been loaded with solid  $\text{KAg}(\text{CN})_2$  (2.269 mg, 11.4  $\mu\text{mol}$ ). The reaction vessel was flame sealed and heated to 120  $^\circ\text{C}$ , where the reaction/crystallization occurred under autogenously generated pressure. After 67 h, the sample vessel was allowed to self-cool to room temperature. The product consisted of yellow crystals of **1** in the form of hexagonal plates. The synthesis of  $\text{Am}[\text{Au}(\text{CN})_2]_3 \cdot 3\text{H}_2\text{O}$  (**2**) was similar to the synthesis of compound **1**, except that  $\text{KAu}(\text{CN})_2$  (3.212 mg, 11.1  $\mu\text{mol}$ ) was used. Crystals of **2** were pink and also consisted of hexagonal plates.

### 2.3. Syntheses of $\text{Nd}[M(\text{CN})_2]_3 \cdot 3\text{H}_2\text{O}$ ( $M = \text{Ag}$ , **3**; $\text{Au}$ , **4**)

The syntheses of compounds **3** and **4** were performed in a manner similar to that described for the americium compounds above. For compound **3**,  $\text{Nd}(\text{NO}_3)_3$  (85.3  $\mu\text{L}$ ,

0.233 M) and  $\text{KAg}(\text{CN})_2$  (11.865 mg, 59.6  $\mu\text{mol}$ ) were reacted, while  $\text{NdCl}_3$  (91.4  $\mu\text{L}$ , 0.225 M) and  $\text{KAu}(\text{CN})_2$  (17.769 mg, 61.7  $\mu\text{mol}$ ) were used in the synthesis of **4**. Crystals in the form of purple hexagonal plates for **3** and **4** were recovered from the reactions as the major solid products. Powder X-ray diffraction experiments revealed the presence of several minor unindexed lines that were not consistent with either the desired products or starting materials. The purity of **3** and **4** was estimated to be  $\sim 95\%$  based on these studies. However, X-ray and spectroscopical studies were conducted on single crystals which provided reproducible results. Average yields for **3** and **4** based on a number of reactions are 55%.

#### 2.4. Single-crystal X-ray diffraction

Single crystals of compounds **1–4** were selected for the X-ray diffraction studies. The crystals of  $\text{Am}[\text{Ag}(\text{CN})_2]_3 \cdot 3\text{H}_2\text{O}$  (**1**) and  $\text{Am}[\text{Au}(\text{CN})_2]_3 \cdot 3\text{H}_2\text{O}$  (**2**) were sealed in quartz capillaries and then placed inside polyethylene tubes used for secondary containment. The crystals of  $\text{Nd}[\text{Ag}(\text{CN})_2]_3 \cdot 3\text{H}_2\text{O}$  (**3**) and  $\text{Nd}[\text{Au}(\text{CN})_2]_3 \cdot 3\text{H}_2\text{O}$  (**4**) were mounted on the tips of quartz fibers. The crystals were aligned on a Bruker SMART APEX CCD X-ray diffractometer with a digital camera. Intensity measurements were performed using graphite monochromated,  $\text{MoK}\alpha$  radiation from a sealed X-ray tube equipped with a monocapillary collimator. The intensities of reflections of a sphere were collected by a combination of three sets of exposure frames. Each set had a different  $\phi$  angle for the crystal, and each exposure covered a range of  $0.3^\circ$  in  $\omega$ . A total of 1800 frames were collected with exposure times per frame of 15 s for **1**, 20 s for **2**, and 30 s for compounds **3** and **4**.

The determination of integrated intensities and a global-cell refinement were performed with the Bruker SAINT (v 6.02) software package using a narrow-frame, integration algorithm. A semi-empirical absorption correction was applied using SADABS [33]. The program suite SHELXTL (v 5.1) was used for space group determination (XPREP), structure solution (XS), and least-squares refinement (XL) [34]. A Patterson function was used to locate the heavy atom positions. The C, N, and O atomic positions were located in difference maps. The hydrogen atoms of the water molecules were not located or calculated. The scattering factor, real and imaginary dispersion terms, and the linear absorption coefficient for americium [35] were manually inputted into the SHELXTL instruction files. The final refinements for **1**, **3**, and **4** included anisotropic displacement parameters for all atoms and a secondary extinction parameter; for **2**, only the americium and gold atoms were refined anisotropically. Experimental challenges included very small crystals coupled with the double containment required for the X-ray experiments, which resulted in a lower quality X-ray structure for **2**. Crystallographic details for compounds **1–4** are listed in Table 1. Further details of the crystal structure investigations may be obtained from the Fachinformationzentrum Karlsruhe, D-76344 Eggenstein-Leopoldshafen, Germany (Fax: (+49)7247-808-666; Email: crysdata@fiz-karlsruhe.de) on quoting the depository numbers CSD-417896 for **1**, CSD-417897 for **2**, CSD-417898 for **3**, and CSD-417899 for **4**.

#### 2.5. Raman spectroscopy

Raman spectroscopy was performed using an argon-ion laser (Coherent, model 306) and a double-meter spectrometer (Jobin-Yvon Ramanor model HG.2S). The resolution

Table 1  
Crystallographic data for  $\text{Am}[\text{Ag}(\text{CN})_2]_3 \cdot 3\text{H}_2\text{O}$  (**1**),  $\text{Am}[\text{Au}(\text{CN})_2]_3 \cdot 3\text{H}_2\text{O}$  (**2**),  $\text{Nd}[\text{Ag}(\text{CN})_2]_3 \cdot 3\text{H}_2\text{O}$  (**3**), and  $\text{Nd}[\text{Au}(\text{CN})_2]_3 \cdot 3\text{H}_2\text{O}$  (**4**)

Formula	$\text{Am}[\text{Ag}(\text{CN})_2]_3 \cdot 3\text{H}_2\text{O}$	$\text{Am}[\text{Au}(\text{CN})_2]_3 \cdot 3\text{H}_2\text{O}$	$\text{Nd}[\text{Ag}(\text{CN})_2]_3 \cdot 3\text{H}_2\text{O}$	$\text{Nd}[\text{Au}(\text{CN})_2]_3 \cdot 3\text{H}_2\text{O}$
Formula mass	776.84	1044.13	678.02	945.31
Color and habit	Yellow, hexagonal plate	Pink, hexagonal plate	Purple, hexagonal plate	Purple, hexagonal plate
Crystal system	Hexagonal	Hexagonal	Hexagonal	Hexagonal
Space group	$P6_3/mcm$ (No. 193)	$P6_3/mcm$ (No. 193)	$P6_3/mcm$ (No. 193)	$P6_3/mcm$ (No. 193)
$a$ (Å)	6.7205(10)	6.666(2)	6.7042(4)	6.6573(13)
$c$ (Å)	18.577(3)	18.342(6)	18.620(1)	18.431(4)
$V$ (Å <sup>3</sup> )	726.64(19)	705.9(4)	724.77(8)	707.2(2)
$Z$	2	2	2	2
$T$ (°C)	21	21	21	21
$\lambda$ (Å)	0.71073	0.71073	0.71073	0.71073
$2\theta_{\text{max}}$	56.58	50.36	56.54	56.54
$\rho_{\text{calcd}}$ (g cm <sup>-3</sup> )	3.551	4.913	3.107	4.440
$\mu$ (MoK $\alpha$ ) (mm <sup>-1</sup> )	9.212	36.463	7.525	34.643
Reflections collected	6567	4793	6464	6247
Independent reflections	360 [ $R(\text{int}) = 0.0406$ ]	254 [ $R(\text{int}) = 0.3069$ ]	360 [ $R(\text{int}) = 0.0266$ ]	350 [ $R(\text{int}) = 0.0520$ ]
Data/restraints/parameters	360/0/24	254/0/15	360/0/24	350/0/24
$R(F)^a$ for $F_o^2 > 2\sigma(F_o^2)^a$	0.0149	0.0404	0.0141	0.0304
$R_w(F_o^2)^b$	0.0371	0.0881	0.0505	0.0677

$$^a R(F) = \frac{\sum ||F_o| - |F_c||}{\sum |F_o|}$$

$$^b R_w(F_o^2) = \left[ \frac{\sum [w(F_o^2 - F_c^2)^2]}{\sum wF_o^4} \right]^{1/2}$$

of the monochromator at 514.5 nm is  $0.5 \text{ cm}^{-1}$ . The monochromator is interfaced with a personal computer; scanning and data collections are controlled by LabSpec (version 3.04) software. Signal detection is acquired with a water-cooled photo-multiplier tube (Hamamatsu R636). The 528 nm wavelength was the principal argon laser line used for excitation in these experiments. The reported spectra are uncorrected for instrumental responses, but the monochromator positions and wavenumber accuracies were calibrated daily using the Hg line at  $18312.7 \text{ cm}^{-1}$  (546.1 nm) from an external source. Additional calibration was conducted using the tri-azaphospha-adamantane ligand (TPA), which exhibits several sharp and intense Raman bands in the region of interest.

## 2.6. Emission spectroscopy

The 514.5 nm line was used for the excitation of the americium complexes. The luminescence spectra were collected using an Instrument SA optical system consisting of a monochromator (model 1000 M) attached to CCD, PMT, and IR detectors. Additional spectra of higher resolution were collected using a HG2.S monochromator. Data analyses were performed with Grams/32 software (Galactic, version 5.1).

## 3. Results and discussion

### 3.1. Material syntheses

Given the limited quantities of americium available, the reaction conditions were first optimized by formation of  $\text{Nd}[M(\text{CN})_2]_3 \cdot 3\text{H}_2\text{O}$  ( $M = \text{Ag}$ (3),  $\text{Au}$ (4)) before the syntheses of  $\text{Am}[M(\text{CN})_2]_3 \cdot 3\text{H}_2\text{O}$  ( $M = \text{Ag}$  (1),  $\text{Au}$  (2)) were attempted. These conditions are given in the experimental section. Initial hydrothermal reactions between  $\text{Nd}(\text{NO}_3)_3$  and  $\text{KAg}(\text{CN})_2$  were attempted at  $170^\circ\text{C}$ , but under these conditions the dicyanoargentate anions decompose, resulting in the reduction of  $\text{Ag}^+$  and formation of silver metal. As determined by single-crystal X-ray characterization,  $\text{Nd}(\text{CO}_3)(\text{OH})$  [36] was also isolated under the above conditions. However, high-quality crystals of compounds 3 or 4 are isolated as the sole crystalline products when  $\text{NdCl}_3$  is reacted with  $\text{KAg}(\text{CN})_2$  or  $\text{KAu}(\text{CN})_2$  in a 1:3 ratio at  $120^\circ\text{C}$ . When  $\text{Nd}(\text{NO}_3)_3$  is reacted with  $\text{KAu}(\text{CN})_2$  at  $120^\circ\text{C}$ ,  $\text{Nd}[\text{Au}(\text{CN})_2]_3 \cdot 3\text{H}_2\text{O}$  is formed as well as an unidentified yellow microcrystalline powder. Reaction times from 16 h to 3 days have been tried and this period was found adequate for the syntheses. Once the synthetic procedures were optimized on the neodymium systems, compounds 1 and 2 were prepared under similar reaction conditions.

Previous reports have outlined the syntheses of similar tris-(dicyanoargentate) lanthanide trihydrates or tris-(dicyanoaurate) lanthanide trihydrates either by slow evaporation [18,26,37] or by gel growth [38] methods. Our synthetic approach for compounds 1–4 was to use the

hydrothermal technique, a method that has also been used recently in the preparation of other transition metal cyanides [39–40]. This method is particularly attractive for the americium systems, and single crystals of  $\text{Am}[M(\text{CN})_2]_3 \cdot 3\text{H}_2\text{O}$  ( $M = \text{Ag}$ (1),  $\text{Au}$ (2)) can be grown with small quantities of reactants (e.g., 0.92 mg Am) in sealed reaction tubes.

### 3.2. Crystal structures

Compounds 1–4 all exhibit the same structure, crystallizing in the hexagonal space group,  $P6_3/mcm$ , and are isostructural to the previously reported  $\text{Eu}[\text{Ag}(\text{CN})_2]_3 \cdot 3\text{H}_2\text{O}$  [26]. This structural type has also been reported for several additional tris(dicyanoargentate)lanthanide trihydrates or tris(dicyanoaurate)lanthanide trihydrates [38,41–42]. Due to the structural similarities of the 1–4 compounds reported here, for brevity, only the structure of  $\text{Am}[\text{Ag}(\text{CN})_2]_3 \cdot 3\text{H}_2\text{O}$  (1) will be discussed in detail; some important comparisons with the other structures will be addressed. Table 1 contains the crystallographic data for these four compounds, and selected bond lengths for compounds 1–4 are given in Tables 2 and 3.

Fig. 1 shows the coordination geometry around the americium atom with the atomic labeling schemes. The environment for the  $\text{Am}^{3+}$  ion in 1 consists of six N-bound  $\text{CN}^-$  groups coordinated approximately end-on in a trigonal prismatic arrangement. In addition, three water molecules cap the rectangular faces of the prism. The resultant tricapped trigonal prismatic coordination environment of the Am site is shown in Fig. 1. The overall cyanide coordination is also shown at one site, but the three-dimensional interaction is clearly evident in the packing diagram shown in Fig. 2. The tricapped trigonal prismatic coordination geometry around the  $\text{Am}^{3+}$  is a  $D_{3h}$

Table 2

Selected bond distances (Å) for  $\text{Am}[\text{Ag}(\text{CN})_2]_3 \cdot 3\text{H}_2\text{O}$  (1), and  $\text{Nd}[\text{Ag}(\text{CN})_2]_3 \cdot 3\text{H}_2\text{O}$  (3)

$\text{Am}[\text{Ag}(\text{CN})_2]_3 \cdot 3\text{H}_2\text{O}$		$\text{Nd}[\text{Ag}(\text{CN})_2]_3 \cdot 3\text{H}_2\text{O}$	
$\text{Am}(1)-\text{N}(1) \times 6$	2.570(5)	$\text{Nd}(1)-\text{N}(1) \times 6$	2.585(2)
$\text{Am}(1)-\text{O}(1) \times 3$	2.496(7)	$\text{Nd}(1)-\text{O}(1) \times 3$	2.478(3)
$\text{C}(1)-\text{N}(1)$	1.132(7)	$\text{C}(1)-\text{N}(1)$	1.134(3)
$\text{Ag}(1)-\text{C}(1) \times 2$	2.072(6)	$\text{Ag}(1)-\text{C}(1) \times 2$	2.059(3)
$\text{Ag}(1) \cdots \text{Ag}(1)'$	3.3603(5)	$\text{Ag}(1) \cdots \text{Ag}(1)'$	3.3521(2)

Table 3

Selected bond distances (Å) for  $\text{Am}[\text{Au}(\text{CN})_2]_3 \cdot 3\text{H}_2\text{O}$  (2) and  $\text{Nd}[\text{Au}(\text{CN})_2]_3 \cdot 3\text{H}_2\text{O}$  (4)

$\text{Am}[\text{Au}(\text{CN})_2]_3 \cdot 3\text{H}_2\text{O}$		$\text{Nd}[\text{Au}(\text{CN})_2]_3 \cdot 3\text{H}_2\text{O}$	
$\text{Am}(1)-\text{N}(1) \times 6$	2.60(3)	$\text{Nd}(1)-\text{N}(1) \times 6$	2.598(7)
$\text{Am}(1)-\text{O}(1) \times 3$	2.51(4)	$\text{Nd}(1)-\text{O}(1) \times 3$	2.479(12)
$\text{Au}(1)-\text{C}(1) \times 2$	2.06(4)	$\text{Au}(1)-\text{C}(1) \times 2$	1.984(10)
$\text{C}(1)-\text{N}(1)$	1.07(5)	$\text{C}(1)-\text{N}(1)$	1.14(1)
$\text{Au}(1) \cdots \text{Au}(1)'$	3.3330(11)	$\text{Au}(1) \cdots \text{Au}(1)'$	3.3287(6)



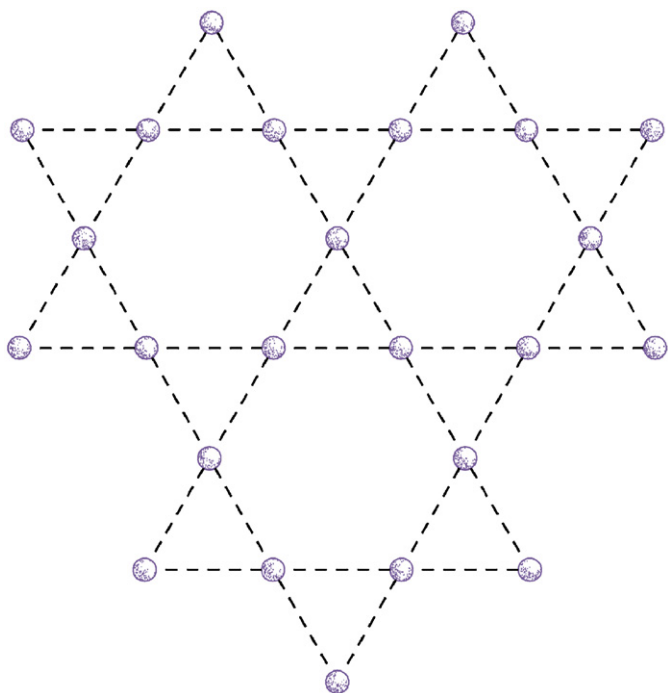


Fig. 3. Drawing showing the Kagomé lattice contained in the structure of compounds **1–4**. Au...Au or Ag...Ag interactions are indicated by the dashed lines. Every Ag or Au atom is surrounded by four other silver or gold atoms placed in a rectangular arrangement.

spectroscopic properties of the complexes. In **2**, the Au...Au separation is slightly smaller (3.3330(11) Å) than the Ag...Ag separation in **1**. When compared with the Am compounds, the  $M...M$  ( $M = \text{Ag}, \text{Au}$ ) distances are smaller for the corresponding neodymium compounds. For example, the Ag...Ag and Au...Au distances are 3.3521(2) and 3.3287(6) Å in the Nd compounds **3** and **4**, respectively. This contributes to the smaller unit cell volumes observed in the gold compounds (~2.6%) as compared with the silver compounds with the same  $f$ -element species (i.e. Am or Nd). Although gold has a higher  $Z$  than silver, the reduction in molecular volume can be traced to the smaller covalent radii arising from the larger “relativistic contraction” for gold [46,47]. Thus, the bonding interactions reflect that, gold is more prone for covalent interaction than silver [48].

### 3.3. Raman studies

The Raman spectra for the silver dicyanide complexes are shown in Fig. 4 in the  $\nu_{\text{CN}}$  stretching region; the band assignments are given in Table 4. As shown in Fig. 4a, the CN symmetric stretch for  $\text{KAg}(\text{CN})_2$  is observed at  $2145\text{ cm}^{-1}$ , consistent with the previously reported value for this compound [49]. Upon coordination with  $\text{Nd}^{3+}$ , the  $\nu_{\text{CN}}$  band blue-shifts by  $\sim 15\text{ cm}^{-1}$  and a single strong band appears at  $2160\text{ cm}^{-1}$ . No significant change is observed on the  $\nu_{\text{CN}}$  symmetric stretching band when neodymium is replaced by the actinide, americium, due to their very

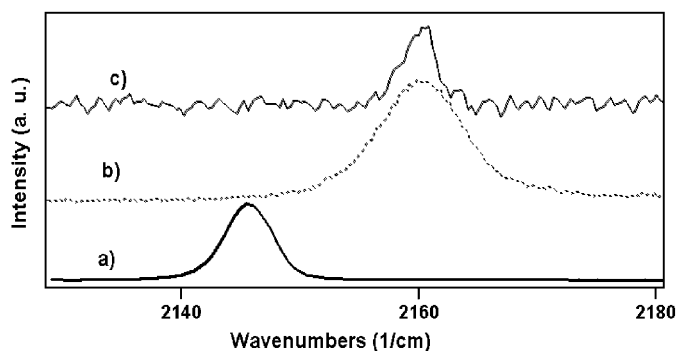


Fig. 4. Raman spectrum of: (a)  $\text{KAg}(\text{CN})_2$ ; (b)  $\text{Nd}[\text{Ag}(\text{CN})_2]_3 \cdot 3\text{H}_2\text{O}$ ; and (c)  $\text{Am}[\text{Ag}(\text{CN})_2]_3 \cdot 3\text{H}_2\text{O}$ .

Table 4  
Assignment of Raman bands ( $\text{cm}^{-1}$ )

$\text{Am}[\text{Au}(\text{CN})_2]_3$	$\text{Nd}[\text{Au}(\text{CN})_2]_3$	$\text{Nd}[\text{Ag}(\text{CN})_2]_3$	Assignment
2176	2166	2160	$\nu(\text{CN})$
	2158		$\nu(\text{CN})$
	491		$\nu(\text{AuC})$
	474		$\nu(\text{AuC})$
		412	$\nu(\text{AgC})$
		384	$\nu(\text{AgC})$
	347		$\delta(\text{AuCN})$
	330		
		308 (sh)	$\delta(\text{AgCN})$
		289	
		274 (sh)	
	226		Lattice modes
	183		Lattice modes
	152		Lattice modes
	120		Lattice modes
	79		$\nu(\text{Au–Au})$

The small size of the americium samples precluded the collection of a reliable data in the low-frequency region.

similar ionic radii. However, the small size of the  $\text{Am}[\text{Ag}(\text{CN})_2]_3 \cdot 3\text{H}_2\text{O}$  crystals results in a weak Raman signal and required a large number of data collection to counter the background noise. The shift of the  $\nu_{\text{CN}}$  to higher energy for compound **3** is consistent with data reported for most cyanometalates that show a blue-shifting upon nitrile binding. This shift can be rationalized as due to a substantial electron density withdrawal from the antibonding N lone pair upon bridging with  $f$ -element ions. Only metals such as Tl and Pb, that participate in back-bonding to the CN group, are known to exhibit red-shifted  $\nu_{\text{CN}}$  symmetric stretching bands [50].

The Raman spectra of the gold dicyanide complexes are shown in Fig. 5 and cover the  $\nu_{\text{CN}}$  stretching region. The spectrum of  $\text{KAu}(\text{CN})_2$  shown in Fig. 5a has a single band at  $2162\text{ cm}^{-1}$ . In the neodymium complex the band splits into two: a strong band at  $2166\text{ cm}^{-1}$  and a much weaker one at  $\sim 2158\text{ cm}^{-1}$  in a ratio of 1:20, respectively. The

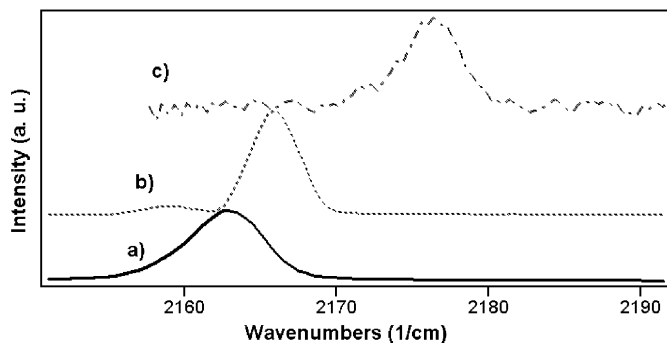


Fig. 5. Raman spectrum of: (a)  $\text{KAu}(\text{CN})_2$ ; (b)  $\text{Nd}[\text{Au}(\text{CN})_2]_3 \cdot 3\text{H}_2\text{O}$ ; and (c)  $\text{Am}[\text{Au}(\text{CN})_2]_3 \cdot 3\text{H}_2\text{O}$ .

spectrum shown in Fig. 5c corresponds to the  $\text{Am}[\text{Au}(\text{CN})_2]_3 \cdot 3\text{H}_2\text{O}$  system, where the  $\nu_{\text{CN}}$  symmetrical stretching band is significantly blue-shifted as compared to either  $\text{KAu}(\text{CN})_2$  or  $\text{Nd}[\text{Au}(\text{CN})_2]_3 \cdot 3\text{H}_2\text{O}$ . This band appears at  $2176 \text{ cm}^{-1}$ . The blue shift in the  $\nu_{\text{CN}}$  stretch indicates bridging of gold and americium, which results in a substantial electron density removal from the cyanide group. When compared with the silver systems, the  $\nu_{\text{CN}}$  frequency appears at a higher energy for the gold dicyanide complexes. The shift to higher frequency is consistent with the structural data where the carbon–nitrogen bond distance is shorter in the gold dicyanide systems. In the Nd–Ag compound the CN bond distance is  $1.134(3) \text{ \AA}$ , with error of the C–N distance of  $1.14(1)$  found in the Nd–Au system. However, the CN bond distance is reduced from  $1.132$  to  $1.07 \text{ \AA}$  on going from the Am–Ag to the Am–Au system, indicating bond strengthening in the latter system.

In the low-energy region, the neodymium compounds provide detailed and well-defined spectral profiles. Although not clearly defined in the  $\text{KAg}(\text{CN})_2$  spectrum (Fig. 6a), the  $\text{Nd}[\text{Ag}(\text{CN})_2]_3 \cdot 3\text{H}_2\text{O}$  system has a well-resolved doublet (Fig. 6b) at  $412$  and  $384 \text{ cm}^{-1}$ , which is assignable to the  $\nu_{\text{Ag-C}}$  stretch. A broad band centering at  $289 \text{ cm}^{-1}$  is also observed with shoulders at  $308$  and  $274 \text{ cm}^{-1}$ , which is blue-shifted compared with that for  $\text{KAg}(\text{CN})_2$  system, (observed at  $249 \text{ cm}^{-1}$ ). These bands are assigned to the Ag–CN bending modes. In the  $\text{Nd}[\text{Au}(\text{CN})_2]_3 \cdot 3\text{H}_2\text{O}$  system, the Au–C stretching appears (Fig. 6d) as a doublet at blue-shifted positions of  $474$  and  $491 \text{ cm}^{-1}$ , when compared with the silver compounds. The blue shift is consistent with a stronger Au–C bond inferred from the M–C distances ( $2.001$  vs.  $2.063 \text{ \AA}$  in Au–C vs. Ag–C, respectively). The Au–CN bending mode in  $\text{Nd}[\text{Au}(\text{CN})_2]_3 \cdot 3\text{H}_2\text{O}$  is also blue-shifted to  $347$  and  $330 \text{ cm}^{-1}$  compared with the values for the Ag–CN modes (Fig. 6b), and the Au–CN bend in  $\text{KAu}(\text{CN})_2$  (Fig. 6c). Additional Raman bands are observed in the lower-energy region at  $226$ ,  $183$ ,  $152$ , and  $120 \text{ cm}^{-1}$ ; all bands are assigned to lattice modes. The much stronger band at  $79 \text{ cm}^{-1}$  is assignable to the Au–Au stretching [51].

Although, it would be desirable to compare the lanthanide Raman data with those for the actinide

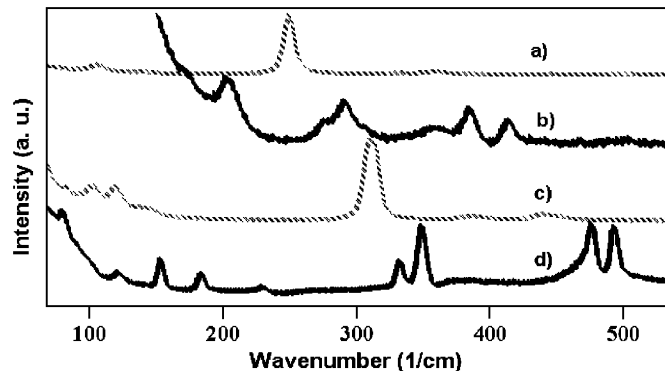


Fig. 6. Raman spectra of the compounds covering the low-energy ( $50$ – $550 \text{ cm}^{-1}$ ) vibrational region: (a)  $\text{KAg}(\text{CN})_2$ ; (b)  $\text{Nd}[\text{Ag}(\text{CN})_2]_3 \cdot 3\text{H}_2\text{O}$ ; (c)  $\text{KAu}(\text{CN})_2$ ; and (d)  $\text{Nd}[\text{Au}(\text{CN})_2]_3 \cdot 3\text{H}_2\text{O}$ .

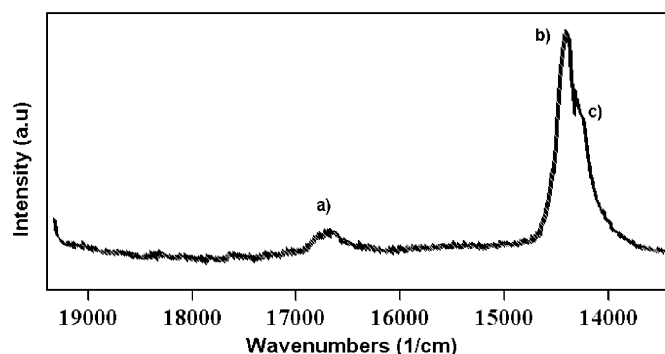


Fig. 7. Emission spectrum of  $\text{Am}[\text{Ag}(\text{CN})_2]_3 \cdot 3\text{H}_2\text{O}$  (1) obtained, using the  $514.5 \text{ nm}$  argon-ion laser line as an excitation source.

complexes, the sample sizes available for analysis combined with the reduced signal intensity in the low-frequency vibrational region limited our ability to collect as suitable Raman data on the americium compounds. However, the structural comparisons indicate that the M–C ( $M = \text{Ag}, \text{Au}$ ) distances in the americium complexes are longer than those of the neodymium systems and a red shift would be anticipated in the  $\nu_{\text{MC}}$  vibrational modes for the Am compounds.

### 3.4. Photoluminescence studies

The photoluminescence spectrum of crystalline  $\text{Am}[\text{Ag}(\text{CN})_2]_3 \cdot 3\text{H}_2\text{O}$  is shown in Fig. 7. The  $514.5 \text{ nm}$  laser line, which is essentially in resonance with the  $^5L_6'$  level, was used to excite the sample. As is evident from the absorption spectrum shown in Fig. 8, the  $^5L_6'$  has the largest absorbance of the  $f$ – $f$  transitions within the americium excited levels. Excitation to this level with the  $514.5 \text{ nm}$  laser line produces emission bands originating from two different excited states. The broad weak band centering at  $\sim 16700 \text{ cm}^{-1}$  corresponds to the  $^5L_6' \rightarrow ^7F_1$  transition [52,53].

The most intense band appears at  $14,350$  with a broad shoulder  $14,250 \text{ cm}^{-1}$ . In this region, americium

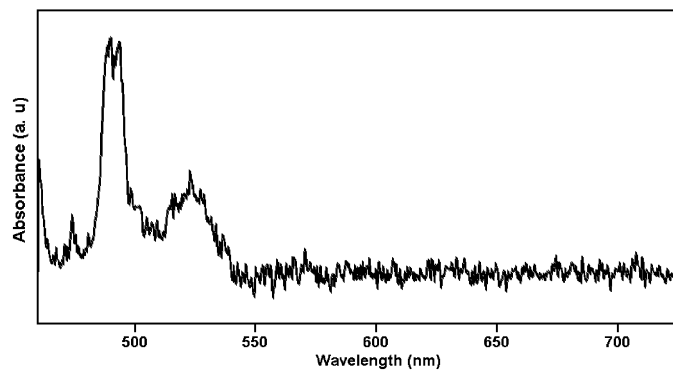


Fig. 8. Solid-state absorption spectrum of a  $\text{Am}[\text{Ag}(\text{CN})_2]_3 \cdot 3\text{H}_2\text{O}$  single crystal. [Absorbance is in arbitrary units.]

luminescence spectra are known of overlapping emissions originating from two different excited levels [52–59]. Based on the established assignments, the higher energy of the emission (with a maximum at  $14350\text{ cm}^{-1}$ ) corresponds to the  $^5D_{1'} \rightarrow ^7F_1$  transitions [54–59], while the lower-energy side mainly corresponds to contributions from the  $^5L_6' \rightarrow ^7F_2'$  transitions. When compared with the americium iodates and borosilicate matrices reported earlier [60–61], the most intense band for the americium emission in the  $\text{Am}[\text{Ag}(\text{CN})_2]_3 \cdot 3\text{H}_2\text{O}$  system is red-shifted by  $250\text{ cm}^{-1}$ . The relative intensities of the emissions from the two excited states are temperature dependent. In the spectrum collected at liquid nitrogen temperature, the lower-energy emission originating from the  $^5L_6'$  state has comparable intensity to that of the higher-energy band corresponding to the  $^5D_{1'} \rightarrow ^7F_1$  transition. The lower-energy band also shows a well-resolved shoulder at  $\sim 14,000\text{ cm}^{-1}$ . The relative decrease of the emission intensity originating from the lower excited state ( $^5D_{1'}$ ) is indicative of the reduced thermal deactivation from the upper  $^5L_6'$  level. The presence of water molecules in the coordination sphere of the Am ion is expected to bridge the gap and facilitate cascading of the excitation to the lower excited level. Radiative transitions from this emitting level to the various ground levels enhances the emission originating from this state.

Several attempts to observe emission from the  $\text{Am}[\text{Au}(\text{CN})_2]_3 \cdot 3\text{H}_2\text{O}$  were not successful, although  $\text{Am}^{3+}$  is one of the strong, spectral-emitting actinide ions. The americium emission in the gold complex is quenched, even at liquid nitrogen temperature, indicating the presence of an intense, non-radiative mechanism responsible for the dissipation of the excitation energy.

#### 4. Summary

The polymeric compounds between americium and gold and silver dicyanides were prepared using a hydrothermal synthetic procedure. Single crystals of  $\text{Am}[M(\text{CN})_2]_3 \cdot 3\text{H}_2\text{O}$  ( $M = \text{Ag}, \text{Au}$ ) were obtained from the reaction of  $\text{AmCl}_3$  and  $M(\text{CN})_2^-$  ( $M = \text{Ag}, \text{Au}$ ) under mild hydrothermal conditions of  $120^\circ\text{C}$ . The americium ion and the

transition metals are interconnected through cyanide bridging.

The isostructural neodymium compounds were prepared for comparison with the americium compounds. All four of these compounds studied crystallize in the same hexagonal space group with only slight differences occurring in their unit cell parameters. The coordination around the Am or Nd consists of six  $\text{CN}^-$  groups coordinated through the N atoms resulting in a trigonal prismatic environment. Three oxygen atoms of coordinated water molecules complete the tricapped trigonal prismatic coordination environment for  $\text{Am}^{3+}$  providing a total coordination number of nine. Raman spectroscopy, which complements the structural work, reveals that all of the compounds display strong signals in the  $\nu_{\text{CN}}$  stretching region. When compared with  $\text{KAg}(\text{CN})_2$  or  $\text{KAu}(\text{CN})_2$ , the  $\nu_{\text{CN}}$  stretching frequency in all the compounds blue-shift due to bridging and substantial electron density removal from the cyanide center. When compared with the silver systems, the  $\nu_{\text{CN}}$  stretching frequency appears at higher energy in the gold dicyanide complexes. The shift to higher frequency is consistent with the structural data where the carbon–nitrogen bond distance decreases in the gold dicyanide systems when compared with the silver system.

#### Acknowledgments

Support for this work was provided by the Division of Chemical Sciences, Geosciences and Biosciences, OBES, USDOE, under Contract DE-AC05-00OR22725 with Oak Ridge National Laboratory, managed by UT-Battelle, LLC. The  $^{243}\text{Am}$  isotope used in these studies was supplied by the USDOE through its production program at ORNL. Dr. Radu Custelcean and Dr. Bruce Moyer at ORNL are thanked for their generous allocation of X-ray diffractometer time. The authors would also like to thank Travis H. Bray at Auburn University for single-crystal X-ray data sets collected on compounds **3** and **4** and Peter Khalifah at the University of Massachusetts for measuring powder X-ray diffraction patterns on compounds **3** and **4**. ZA also acknowledges the support from the National Oceanic and Atmospheric Administration Educational Partnership Program (NOAA-EPP) Award no. NA06OAR4810187 to North Carolina A&T State University.

#### References

- [1] L.R. Hanton, C.A. Hunter, D.H. Purvis, J. Chem. Soc., Chem. Commun. (1992) 1134.
- [2] H. Bock, R. Dienelt, H. del-Scho, Z. Havlas, J. Chem. Soc., Chem. Commun. (1993) 1792.
- [3] S. Subramanian, M.J. Zaworotko, J. Chem. Soc., Chem. Commun. (1993) 952.
- [4] C.M. Drain, R. Fischer, E.G. Nolen, J.M. Lehn, J. Chem. Soc. Chem. Commun. (1993) 243.
- [5] J.M. Lehn, M. Mascal, A. DeCian, J. Fischer, J. Chem. Soc., Chem. Commun. (1990) 479.
- [6] K.R. Dunbar, R.A. Heintz, Prog. Inorg. Chem. 45 (1997) 283.
- [7] M. Verdaguier, Science 272 (1996) 698.

- [8] S. Ferlay, T. Mallah, R. Ouahes, P. Veillet, M. Verdaguer, *Nature* 378 (1995) 701.
- [9] M. Verdaguer, A. Bleuzen, V. Marvaud, J. Vaissermann, M. Seuleiman, C. Desplanches, A. Sculler, C. Train, R. Garde, G. Gelly, C. Lomenech, I. Rosenman, P. Veillet, C. Cartier, F. Villain, *Coord. Chem. Rev.* 190 (1999) 1023.
- [10] M. Ohba, K. Okawa, *Coord. Chem. Rev.* 198 (2000) 313.
- [11] A. Figuerola, C. Diaz, M.S. El Fallah, J. Ribas, M. Maestro, J. Mahia, *J. Chem. Commun.* 0 (2001) 1204.
- [12] C.E. Plecnik, L. Shengming, S.G. Shore, *Acc. Chem. Res.* 36 (2003) 499.
- [13] I. Muga, J.M. Gutierrez-Zorrilla, P. Vitoria, P. Roman, L. Lezama, J.I. Beitia, *Eur. J. Inorg. Chem.* (2004) 1886.
- [14] B.-H. Xia, C.-M. Che, D.L. Phillips, K.-H. Leung, K.-K. Cheung, *Inorg. Chem.* 41 (2002) 3866.
- [15] K. Angermaier, E. Zeller, H. Schmidbaur, *J. Organomet. Chem.* 472 (1–2) (1994) 371.
- [16] J.M. Forward, J.P. Fackler Jr., Z. Assefa, in: D.M. Roundhill, J.P. Fackler Jr. (Eds.), *Optoelectronic Properties of Inorganic Compounds*, Plenum Press, New York, 1999, pp. 195–229.
- [17] H.H. Patterson, G. Roper, J. Bischof, A. Ludi, N. Blom, *J. Lumin.* 31/32 (1984) 555.
- [18] Z. Assefa, G. Shankle, R. Reynolds, H.H. Patterson, *Inorg. Chem.* 33 (1994) 2187.
- [19] Z. Assefa, B.G. McBurnett, R.J. Staples, J.P. Fackler Jr., B. Assman, K. Angermaier, H. Schmidbaur, *Inorg. Chem.* 34 (1995) 75.
- [20] M.A. Omary, H.H. Patterson, *J. Am. Chem. Soc.* 120 (1998) 7696.
- [21] M.A.O. Rawashdeh, M.A. Omary, H.H. Patterson, J.P. Fackler Jr., *J. Am. Chem. Soc.* 123 (2001) 11237.
- [22] Z. Assefa, B.G. McBurnett, R.J. Staples, J.P. Fackler Jr., *Inorg. Chem.* 34 (1995) 4965.
- [23] I.K. Chu, I.P.Y. Shek, K.W.M. Siu, W.-T. Wong, J.-L. Zuo, T.-C. Lau, *New J. Chem.* 24 (2000) 765.
- [24] W.-F. Yeung, W.-T. Wong, J.-L. Zuo, T.-C. Lau, *J. Chem. Soc., Dalton Trans.* 0 (2000) 629.
- [25] A. Stier, K.-J. Range, *Z. Naturforsch.* 51b (1996) 698.
- [26] Z. Assefa, R.J. Staples, J.P. Fackler Jr., H.H. Patterson, G. Shankle, *Acta Crystallogr. C* 51 (1995) 2527.
- [27] D.J. Chesnut, D. Plewak, J. Zubieta, *J. Chem. Soc., Dalton Trans.* (2001) 2567.
- [28] D.J. Chesnut, A. Kusnetzow, R. Birge, J. Zubieta, *J. Chem. Soc., Dalton Trans.* (2001) 2581.
- [29] E. Colacio, J.M. D-Vera, F. Lloret, J.M.M. Sanchez, R. Kivekas, A. Rodriguez, R. Sillanpaa, *Inorg. Chem.* 42 (2003) 4209.
- [30] M.J. Katz, P.M. Aguiar, R.J. Batchelor, A.A. Bokov, Z.-G. Ye, S. Kroeker, D.B. Leznoff, *J. Am. Chem. Soc.* 128 (2006) 3669.
- [31] G.B. Andreev, M.Y. Antipin, A.M. Fedoseev, N.A. Budantseva, *Kristallografiya* 46 (3) (2001) 433–434 (Moscow, Russia).
- [32] G.A. Shagisultanova, N.N. Kuznetsova, *Russian J. Coordin. Chem.* (Translation of *Koordinatsionnaya Khimiya*) 29 (10) (2003) 703–709.
- [33] SADABS. Program for absorption correction using SMART CCD based on the method of Blessing: R. H. Blessing, *Acta Crystallogr. A* 51 (1995) 33.
- [34] G. M. Sheldrick, SHELXTL PC, Version 5.0, An integrated system for solving, refining, and displaying crystal structures from diffraction data; Siemens Analytical X-ray Instruments Inc., Madison, WI, 1994.
- [35] A. J. C. Wilson, *International Tables for Crystallography*, vol. C, Mathematical, Physical and Chemical Tables, Kluwer Academic Publishers, Boston, 1992.
- [36] H. Dexpert, P. Caro, *Mater. Res. Bull.* 9 (1974) 1577.
- [37] H. Yersin, D. Trümbach, J. Strasser, H.H. Patterson, Z. Assefa, *Z. Inorg. Chem.* 37 (1998) 3209.
- [38] J.C.F. Colis, C. Larochele, R. Staples, R. Herbst-Irmer, H.H. Patterson, *Dalton Trans.* (2005) 675.
- [39] S.J. Hibble, S.G. Eversfield, A.R. Cowley, A.M. Chippindale, *Angew. Chem. Int. Ed.* 43 (2004) 628.
- [40] T. Pretsch, I. Brüdgam, H. Hartl, *Z. Anorg. Allg. Chem.* 630 (2004) 353.
- [41] J.C.F. Colis, R.J. Staples, C. Tripp, D. Labrecque, H.H. Patterson, *J. Phys. Chem. B* 109 (2005) 102.
- [42] P.A. Tanner, X. Zhou, W.-T. Wong, C. Kratzer, H. Yersin, *J. Phys. Chem. B* 109 (2005) 13083.
- [43] J.H. Burns, W.H. Baldwin, *Inorg. Chem.* 16 (1977) 289.
- [44] Y. Akimoto, *J. Inorg. Nucl. Chem.* 29 (1967) 2650.
- [45] M. J. Jensen, T. E. Albrecht-Schmitt, unpublished results.
- [46] P. Pyykko, *Angew. Chem. Int. Ed.* 43 (2004) 4412.
- [47] P. Pyykko, *Inorg. Chim. Acta* 358 (2005) 4113.
- [48] A. Bayler, A. Schier, G.A. Bowmaker, H. Schmidbauer, *J. Am. Chem. Soc.* 118 (1996) 7006.
- [49] H. Stammerich, B. Chadwick, S. Frankiss, *J. Mol. Struct.* 1 (1967) 191.
- [50] M.J. Katz, P.M. Aguiar, R.J. Batchelor, Z.-G. Ye, S. Kroeker, D.B. Leznoff, *J. Am. Chem. Soc.* 128 (9) (2006) 3669.
- [51] D. Perreault, M. Drouin, A. Michel, V.M. Miskowski, W.P. Schaefer, P.D. Harvey, *Inorg. Chem.* 31 (1992) 695.
- [52] R.W. Valenzuela, R.T. Brundage, *J. Chem. Phys.* 93 (1990) 8469.
- [53] J.V. Beitz, R.T. Brundage, *J. Alloy Compd.* 181 (1992) 49.
- [54] M. Williams, R.T. Brundage, *Phys. Rev. B* 45 (1992) 4561.
- [55] M. Shiloh, M. Givon, Y. Marcus, *J. Inorg. Nucl. Chem.* 31 (1969) 1807.
- [56] D.E. Henrie, R.L. Fellows, G.R. Choppin, *Coord. Chem. Rev.* 18 (1976) 199.
- [57] S. Hubert, P. Thouvenot, N. Edelstein, *Phys. Rev. B* 48 (1993) 5751.
- [58] G.P. Chudnovskaya, Y.I. Gavrish, Y.A. Barbanel, *Radiochimica* 30 (1988) 46.
- [59] G.P. Chudnovskaya, R.B. Dushin, V.V. Kolin, Y.A. Barbanel, *Radiochimica* 27 (1985) 545.
- [60] R.E. Sykora, Z. Assefa, R.G. Haire, T.E. Albrecht-Schmitt, *Inorg. Chem.* 44 (2005) 5667.
- [61] Z. Assefa, R.G. Haire, N. Stump, *J. Nuc. Sci. Technol. Suppl.* 3 (2002) 132.